New derivation of redshift distance without using power expansions

Steffen Haase[*1]

[*]Leipzig, Germany

Abstract

Here we use the flat Friedmann-Lemaitre-Robertson-Walker metric describing a spatially homogeneous and isotropic universe to derive the cosmological redshift distance in a way which differs from that which can be found in the astrophysical literature.
We use the co-moving coordinate r_e (the subscript **e** indicates **e**mission) for the place of a galaxy which is emitting photons and r_a (the subscript **a** indicates **a**bsorption) for the place of an observer within a different galaxy on which the photons - which were traveling thru the universe - are absorbed. Therefore the real physical distance - the way of light - is calculated by $D = a(t_0)\, r_a - a(t_e)\, r_e$. Here means $a(t_0)$ the today's (t_0) scale parameter and $a(t_e)$ the scale parameter at the time of emission (t_e) of the photons. Nobody can doubt this real travel way of light: The photons are emitted on the co-moving coordinate place r_e and are than traveling to the co-moving coordinate place r_a. During this traveling the time is moving from t_e to t_0 ($t_e \leq t_0$) and therefore the scale parameter is changing in the meantime from $a(t_e)$ to $a(t_0)$.
Using this right way of light we calculate some relevant classical cosmological equations (effects) and compare these theoretical results with some measurements of astrophysics. As one result we get e.g. the today's Hubble parameter $H_{0a} \approx 62.34$ km/(s Mpc). This value is smaller than the Hubble parameter $H_{0,Planck} \approx 67.66$ km/(s Mpc) resulting from *Planck 2018 data* [12] which is discussed in the literature.

Key words: relativistic astrophysics, theoretical and observational cosmology, redshift, Hubble parameter, quasar

PACS NO:

[1] steffen_haase@vodafone.de

Contents:

List of Figures:

List of Tables:

1. Introduction

The current cosmological standard model assumes the correctness of Einstein's field equations (EFE) containing the cosmological term Λ

$$G_{\mu\nu} = \frac{8\pi G}{c^4} T_{\mu\nu} - \Lambda g_{\mu\nu} \tag{1}$$

and solves this with the help of the Friedmann-Lemaitre-Robertson-Walker metric (FLRWM)

$$ds^2 = c^2 dt^2 - a^2(t)\left[\frac{dr^2}{1-\varepsilon r^2} + r^2(d\vartheta^2 + \sin^2\vartheta d\varphi^2)\right] \quad , \tag{2}$$

which is suitable for the description of a homogeneous and isotropic universe evolving over time.

The solutions found by solving the EFE are the Friedmann equations (FE)

$$\left(\frac{\dot{a}}{a}\right)^2 = \frac{8\pi G}{3}\rho - \frac{\varepsilon c^2}{a^2} + \frac{\Lambda c^2}{3} \qquad \textit{and} \qquad \frac{\ddot{a}}{a} = -\frac{8\pi G}{3}\left(\rho + \frac{3P}{c^2}\right) + \frac{\Lambda c^2}{3} \quad . \tag{3}$$

$G_{\mu\nu}$ is the Einstein tensor, G the gravitational constant, $T_{\mu\nu}$ the energy-momentum tensor and Λ the cosmological constant that Einstein added to his original field equations, but later discarded. With ε = 0, +1 or -1 the constant of curvature was introduced and r, ϑ and φ are spherical polar coordinates. The time-dependent scale parameter was designated with a(t) and its time derivatives with points above. P is the pressure of matter and ρ is its density.

Both FE together lead to the law of conservation of energy

$$\frac{d}{dt}a^3\rho c^2 + P\frac{d}{dt}a^3 = 0 \quad , \tag{4}$$

which for pressure less matter then turns into a law of conservation of mass because of P = 0:

$$\frac{d}{dt}a^3\rho c^2 = 0 \qquad \textit{or} \qquad a^3\rho \propto M = const \qquad \textit{because of} \qquad \rho \propto \frac{M}{a^3} \tag{5}$$

This mass M contains all matter that is gravitationally effective in the universe.
In practice, due to the existence of the conservation law, only the first of the two Friedmann equations (3) is usually used.

1.1 Simplifying assumptions

The application of the theoretical standard cosmology to the measured data of the observational cosmology shows that the universe is flat. For this reason, the curvature constant ε is negligible. We agree with this finding, whereby the FLRWM and the FE simplify to

$$ds^2 = c^2 dt^2 - a^2(t)\left[dr^2 + r^2(d\vartheta^2 + \sin^2\vartheta d\varphi^2)\right] \tag{2a}$$

and

$$\left(\frac{\dot{a}}{a}\right)^2 = \frac{8\pi G}{3}\rho + \frac{\Lambda c^2}{3} \quad , \tag{3a}$$

respectively.

The standard cosmology uses the following density parameters $\Omega_{0,\,i}$ (i = M, R, Λ) for the different types of matter that may exist in the universe

$$\Omega_{0,M} = \frac{\rho_{0,M}}{\rho_{0,k}} \qquad \Omega_{0,R} = \frac{\rho_{0,R}}{\rho_{0,k}} \qquad \Omega_{0,\Lambda} = \frac{\rho_{0,\Lambda}}{\rho_{0,k}} \tag{6}$$

$$\textit{with} \qquad \rho_{0,k} \equiv \frac{3H_0^{\,2}}{8\pi G} \approx 1{,}878 * 10^{-29}\ h^2\ g/cm^3$$

and determines their values using measurement data from observing cosmology. With $\rho_{0,\,M}$ today's density (first index 0) of the non-relativistic matter was introduced and $\rho_{0,\,R}$ describes the today's density of the relativistic matter, e.g. radiation (index R). A today's density $\rho_{0,\Lambda}$ is assigned to the cosmological constant Λ and the today's so-called critical density is defined with $\rho_{0,\,k}$, which - neglecting the cosmological constant - corresponds to an equilibrium between kinetic energy ($da/dt \neq 0$) and potential energy of gravitation. H_0 is today's Hubble parameter. The dimensionless parameter h scales the Hubble parameter.

The evaluation of the measurement data using standard cosmology shows that today's quotient of $\rho_{0,R}/\rho_{0,M}$ being

$$\frac{\Omega_{0,R}}{\Omega_{0,M}} = \frac{\rho_{0,R}}{\rho_{0,M}} \approx \frac{8{,}5 * 10^{-5}}{0{,}3} \approx 2{,}83 * 10^{-4} \tag{6a}$$

is very small, which is why today's radiation density $\rho_{0,R}$ can be neglected compared to today's non-relativistic matter density $\rho_{0,M}$. We make use of this knowledge when deriving the redshift distance.

In the following, we also neglect the mathematical possible cosmological constant Λ. The comparison of the redshift distance derived here with measurement results shows in retrospect that this additional parameter is not required. As a result, the EFE are returned to their historically original form and the FE takes on the simpler form

$$\left(\frac{\dot{a}}{a}\right)^2 = \frac{8\pi G}{3}\rho \quad . \tag{3b}$$

2 Derivation of cosmological relevant relations

2.1 Previews

From the requirement of homogeneity it follows that all extra-galactic objects remain at their coordinate location r in the course of the temporal development of the universe, i.e. the coordinate distance between randomly selected galaxies does not change over time, the galaxies rest in this coordinate system. For this reason, dr/dt = 0 applies to them.
This does not apply to the freely moving photons in the universe: They detach themselves from a galaxy at a certain point in time at a certain coordinate location, and are then later absorbed at a completely different coordinate location. In addition, the time-dependent scale parameter a(t) changes between the two points in time which stretches all real physical distances if a cosmic expansion exists.

Here we introduce the designation $r_{\mathbf{e}}$ (the subscript **e** indicates **e**mission of light) for the coordinate location of the light-emitting galaxy and name the coordinate location of the galaxy in which the observer resides $r_{\mathbf{a}}$ (the subscript **a** indicates **a**bsorption of light). In the Euclidean space (ε = 0) considered here, both variables mark the coordinate distance from the coordinate origin r = 0. The constant coordinate distance between the two galaxies is therefore calculated to be $r_a - r_e$ if we assume that the galaxy of the observer is more depart from the coordinate origin as the light-emitting galaxy. The light should therefore move from the inside to the outside within a spherical assumed mass distribution (outgoing photons), which serves as a simple model for the universe (using the FLRWM, it is quite easy to arrange that all directions are of a radial kind).

Due to the measurable expansion of the universe we know that in the course of cosmic evolution all physical distances over the time-dependent scale parameter a(t) being stretched according to the FE (3b).
Then the conservation law for the product of the density of matter ρ(t) and the cube of the scale parameter a(t)

$$\rho a^3 = A \tag{7}$$

also applies. This means that A is a constant which essentially corresponds to the mass of the visible part of the universe (here called the Friedmann sphere). Because of A = constant Eq. (7) can also be written as

$$A = \rho(t_0)\, a^3(t_0) = \rho(t_e)\, a^3(t_e) = \rho_0 {a_0}^3 = \rho_e {a_e}^3 \quad , \tag{8}$$

where ρ_e and ρ_0 denote the densities of the universe and a_e and a_0 are the scale parameters at two different times t_e (time point of **e**mission) and t_0 (today's time point of absorption), respectively. Using Eq. (7) the FE (3b) yields

$$\left(\frac{da}{dt}\right)^2 = \frac{8\pi G}{3}\frac{A}{a} = \frac{B}{a} \quad . \tag{9}$$

With B another constant was introduced which just summarizes other constants. Using the law of mass conservation (7) means also that the mass of the universe which is inside a Friedmann sphere with the current "radius" a(t) is responsible for the expansion. This applies to all points of time. "Radius" (in quoted marks) was written here because a(t) does not have the meaning of a real physical radius. Only the product of the co-moving radial coordinate r and the scale parameter a(t) has this significance, as we shall see immediately.

For a galaxy resting in the coordinate system of the FLRWM, the real physical distance from the coordinate origin becomes calculated to

$$R(t) = a(t)\int_0^r \frac{dr}{\sqrt{1-\varepsilon r^2}} = a(t)\, r \quad , \tag{10}$$

if ε = 0 is considered. The co-moving coordinate r does not depend on time for galaxies.

The physical distance of the light-emitting galaxy from the coordinate origin at time t_e is therefore

$$R_e(t_e) = a(t_e)\, r_e \equiv a_e r_e \quad , \tag{11}$$

while for the analog distance of the galaxy containing the observer at the same time

$$R_a(t_e) = a(t_e)\, r_a \equiv a_e r_a \tag{12}$$

applies. The physical distance of both galaxies at the time t_e is therefore

$$D(t_e) = D_e = a_e r_a - a_e r_e = a_e\left(r_a - r_e\right) \quad . \tag{13}$$

For the distance between both cosmic objects at a later time - means today's time here - $t_0 > t_e$ then applies

$$D(t_0) = D_0 = a_0 r_a - a_0 r_e = a_0\left(r_a - r_e\right) \quad . \tag{14}$$

However, both distances mentioned above are worthless for the computation of cosmological relevant relations, since the emitted photons make their way to the observer, which has to be calculated in accordance with

$$D = a_0 r_a - a_e r_e \quad . \tag{15}$$

To see this, imagine a photon that detaches itself at the time $t_e < t_0$ from the emitting galaxy at the coordinate r_e, where the scale parameter at this time has the value a_e. After the photon has moved freely through the universe, it will arrive at the coordinate point r_a, the place of the observer within another galaxy, at time t_0, with the scale parameter at that time being a_0. Thus, the photon does not travel the path described by Eq. (13) nor by Eq. (14). The real distance traveled by the photon is always greater than any one of these distances. This must be taken into account when deriving the redshift distance.

The real physical light path is illustrated by the green line in Fig 1.:

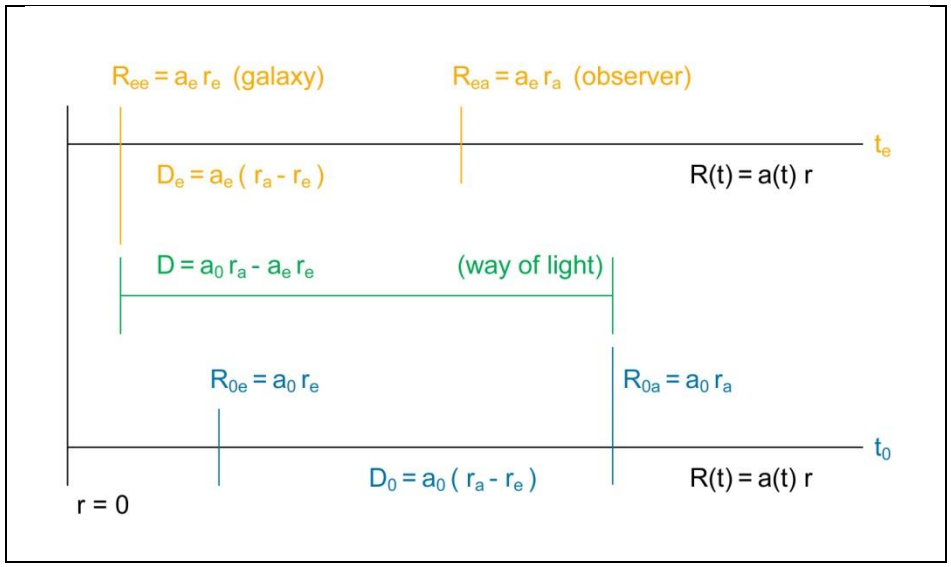

Figure 1. Real physical light path

These remarks may be sufficient as a preliminary to the now following derivation of the redshift distance.

2.2 The redshift distance

We now want to investigate which equation results for the redshift distance (corresponding to the photon path), which depends on the redshift z, if the integral

$$\int_{r_e}^{r_a} dr = +\int_{t_e}^{t_0} \frac{c\,dt}{a(t)} \tag{16}$$

is used. This integral results for $\varepsilon = 0$ when the line element ds is set equal to zero in the FLRWM (2a) and radial ($\vartheta = \varphi = 0$) outgoing photons are considered. Eq. (16) describes the motion of photons in the universe traveling from the coordinate r_e to the coordinate r_a.

During the travel time of the photons, the scale parameter changes from a_e to a_0. If the time differential is replaced using the FE (9), follows from Eq. (16)

$$\int_{r_e}^{r_a} dr = \frac{c}{\sqrt{B}} \int_{a_e}^{a_0} \frac{da}{\sqrt{a}} \quad . \tag{17}$$

After the execution of the integral we get

$$r_a - r_e = \frac{2c}{\sqrt{B}} \left(\sqrt{a_0} - \sqrt{a_e} \right) \quad . \tag{18}$$

Here we multiply both sides with a_0 and at the same time we extract the root of a_0 from the parenthesis:

$$a_0 r_a - a_0 r_e = \frac{2c}{\sqrt{B}} a_0^{3/2} \left(1 - \sqrt{\frac{a_e}{a_0}} \right) \quad . \tag{19}$$

On the left side of Eq. (19) is not yet the real path traveled by the photon, but the today's physical distance of the two galaxies involved.

We now introduce the redshift. To this end, we recall the simple relation between the scale parameters at two different times t_e and t_0 and the redshift z

$$\frac{a_0}{a_e} = 1 + z \qquad or \qquad \frac{a_e}{a_0} = \frac{1}{(1+z)} \tag{20a, b}$$

and also

$$a_0 = (1+z) a_e \quad . \tag{20c}$$

If Eq. (20b) is inserted into Eq. (19), the result is

$$a_0 r_a - a_0 r_e = \frac{2c}{\sqrt{B}} a_0^{3/2} \left(1 - \frac{1}{\sqrt{1+z}} \right) \quad . \tag{21}$$

Next, all unknown variables have to be eliminated from Eq. (21). First, we use the conservation law (8) in connection with Eq. (9) to eliminate a_0 on the right side of Eq. (21). The result is

$$a_0 r_a - a_0 r_e = \frac{2c}{\sqrt{\frac{8\pi G \rho_0}{3}}} \left(1 - \frac{1}{\sqrt{1+z}} \right) \quad , \tag{22}$$

where ρ_0 describes today's mass density of the universe.

For further derivation of the redshift distance, we now take into consideration the Eq. (20c)

$$a_0 r_a - (1+z) a_e r_e = \frac{2c}{\sqrt{\frac{8\pi G \rho_0}{3}}} \left(1 - \frac{1}{\sqrt{1+z}} \right) \tag{23}$$

to use then the light path D introduced by Eq. (15)

$$a_e r_e = a_0 r_a - D \tag{15a}$$

to get

$$a_0 r_a - (1+z)(a_0 r_a - D) = \frac{2c}{\sqrt{\frac{8\pi G \rho_0}{3}}} \left(1 - \frac{1}{\sqrt{1+z}} \right) \quad . \tag{24}$$

The further calculation results from suitable step-wise putting outside the brackets and summarization

$$a_0 r_a - (1+z)\, a_0 r_a + (1+z)\, D = \frac{2c}{\sqrt{\frac{8\pi G \rho_0}{3}}}\left(1 - \frac{1}{\sqrt{1+z}}\right) \tag{25}$$

and

$$-a_0 r_a z + (1+z)\, D = \frac{2c}{\sqrt{\frac{8\pi G \rho_0}{3}}}\left(1 - \frac{1}{\sqrt{1+z}}\right) \quad , \tag{26}$$

respectively.

$$(1+z)\, D = \frac{2c}{\sqrt{\frac{8\pi G \rho_0}{3}}}\left(1 - \frac{1}{\sqrt{1+z}}\right) + a_0 r_a z \quad . \tag{27}$$

Now we put $a_0 r_a$ outside the brackets on the right side of Eq. (27), which results in

$$(1+z)\, D = a_0 r_a \left[\frac{2c}{a_0 r_a \sqrt{\frac{8\pi G \rho_0}{3}}}\left(1 - \frac{1}{\sqrt{1+z}}\right) + z\right] \quad . \tag{28}$$

We introduce $D_{0a} = a_0 r_a$ as an abbreviation for the present physical location of the observer and solve Eq. (28) for D

$$D = \frac{D_{0a}}{(1+z)}\left[\frac{2c}{D_{0a} \sqrt{\frac{8\pi G \rho_0}{3}}}\left(1 - \frac{1}{\sqrt{1+z}}\right) + z\right] \quad . \tag{29}$$

As a further abbreviation we use

$$\frac{1}{\beta_0} = \frac{2c}{D_{0a} \sqrt{\frac{8\pi G \rho_0}{3}}} = \frac{c}{V_0} \tag{30}$$

resulting in

$$D(z; D_{0a}, \beta_0) = \frac{D_{0a}}{(1+z)}\left[\frac{1}{\beta_0}\left(1 - \frac{1}{\sqrt{1+z}}\right) + z\right] \quad . \tag{31}$$

The redshift distance D is therefore a function of z and the two parameters D_{0a} and β_0, which both can be determined by fitting the equation to the astrophysical measurements.
The name β_0 was chosen for the second parameter because it is a today's quotient of two velocities, where the denominator is the speed of light named c.

The literature does not know the parameter β_0. It results from the non-zeroing of r_a for the observer or of $r_e \neq 0$ for the observed galaxy.

For $\beta_0 = 1$, the simpler equation results

$$D(z; D_{0a}, \beta_0 = 1) = D_{0a}\left(1 - \frac{1}{(1+z)^{3/2}}\right) \quad . \tag{31a}$$

The expansion of Eq. (31) for small redshifts z leads to

$$D \approx \left(\frac{1}{2\beta_0} + 1\right) D_{0a} z \quad . \tag{32}$$

If this equation is solved for z and then multiplied by c, the result is

$$c\,z \approx \frac{c}{\left(\frac{1}{2\beta_0} + 1\right)} \frac{D}{D_{0a}} \quad . \tag{33}$$

That is how we find today's Hubble parameter

$$H_{0a} = \frac{c}{\left(\frac{1}{2\beta_0} + 1\right) D_{0a}} \quad . \tag{34}$$

The Hubble parameter also depends on the speed quotient β_0 introduced above and is in this form valid only for small redshifts because of the series expansion. This means that this H_{0a} is only valid locally.

For parameter $\beta_0 = 1$ we get

$$H_{0a} = \frac{2c}{3D_{0a}} \quad . \tag{34a}$$

The reciprocal of this is the Hubble time for $\beta_0 = 1$:

$$t_{H_{0a}} = \frac{3D_{0a}}{2c} \tag{34b}$$

We now give another expression for $1/\beta_0$

$$\frac{2c}{D_{0a}\sqrt{\frac{8\pi G \rho_0}{3}}} = 2\sqrt{\frac{D_{0a}}{R_S}} = \frac{1}{\beta_0} \quad , \tag{35}$$

which results from the Eq. (7) and Eq. (8)

$$M = \frac{4\pi}{3} A r_a^{\,3} = \frac{4\pi}{3} \rho_0 a_0^{\,3} r_a^{\,3} = \frac{4\pi}{3} \rho_0 D_{0a}^{\,3} \quad . \tag{36}$$

With $R_S = 2MG / c^2$, the Schwarzschild radius of mass M of the Friedmann sphere was introduced for pure formal reason. It does not play the same role here as it does within the Schwarzschild metric.

For $\beta_0 = ½$ we get $D_{0a} = R_S$. In this case we could believe that every observer is on the surface of a black hole (corresponds to the Friedmann sphere) and that he always looks into a black hole while observing. For a galaxy

located in the center of the Friedmann sphere, an observer would measure an infinitely large redshift. Overall, that could be logical.

For $\beta_0 = 1$, $D_{0a} = R_S / 4$ would result and the speed V_0 would be exactly identical to the speed of light c.

The mass M contains all gravitational effective components of the visible universe: $M = \sum M_i$. These can also be different energy components E_i, to which, according to Einstein's energy-mass relationship $M_i = E_i/c^2$, masses M_i can be assigned. In addition, with M as the total mass, mass components that are invisible to us (perhaps only so far) are taken in to consideration.

With the help of Eq. (35) the Eq. (31) can be rewritten as

$$D(z; D_{0a}, R_S) = \frac{D_{0a}}{(1+z)}\left[2\sqrt{\frac{D_{0a}}{R_S}}\left(1-\frac{1}{\sqrt{1+z}}\right)+z\right] \quad . \tag{31b}$$

If the comparison with the measurement data shows $\beta_0 = 1$, we would get

$$D(z; R_S) = \frac{R_S}{4}\frac{1}{(1+z)}\left[\left(1-\frac{1}{\sqrt{1+z}}\right)+z\right]$$

because of

$$\frac{1}{\beta_0} = 1 = 2\sqrt{\frac{D_{0a}}{R_S}} \qquad or \qquad D_{0a} = \frac{R_S}{4} \quad .$$

This means

$$D(z; R_S) = \frac{R_S}{4}\left[1-\frac{1}{(1+z)\sqrt{1+z}}\right] \quad . \tag{31c}$$

In this case, we immediately see that the total mass M of the Friedmann sphere goes directly into the equation in the form of the formally introduced Schwarzschild radius R_S. Therefore, it can be used as a scale of cosmological distances.

Fig. 2. shows the redshift distance (31) normalized to the distance D_{0a} for various values of the parameter β_0.

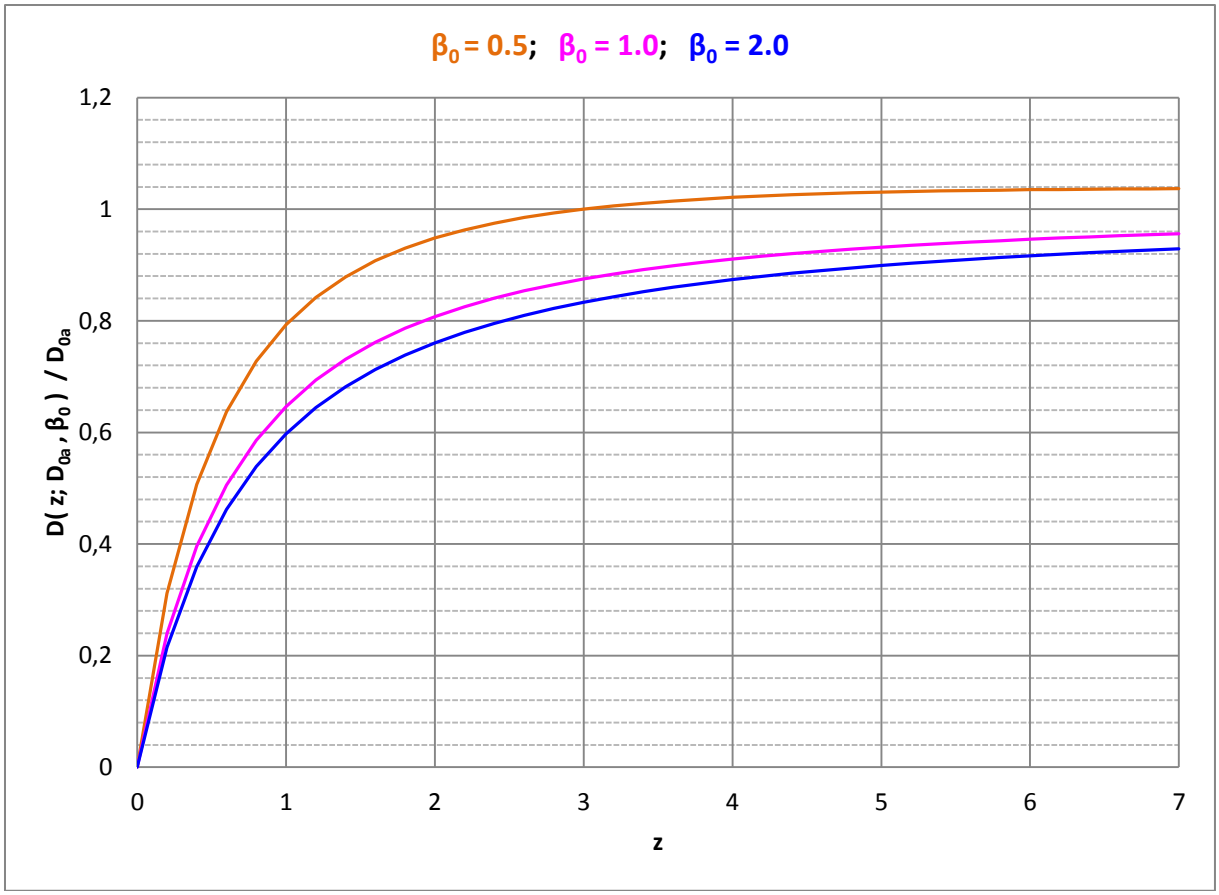

Figure 2. Redshift distance for different values of the parameter β_0

The curvature of the curves is a direct consequence of the Friedmann equation.

For $\beta_0 = 1$, the distance $D = D_{0a}$ is achieved for $z = \infty$.
As a reminder: D_{0a} is today's distance of the observer from the origin of the coordinate system, who is placed on the surface of "his" Friedmann sphere.

The comparison of Eq. (31b) with a Hubble diagram thus determines the current radius $D_{0a} = a_0 r_a$ of the Friedmann sphere (today's physical location of the observer) and its Schwarzschild radius R_S.

Overall, each observer is located on the surface of all imaginable Friedmann spheres around him (for each viewing direction a Friedmann sphere with the radius D_{0a} belongs). The extragalactic objects (placed on $r = r_e$) observed by him then all lie according to their redshift z on a radial line somewhere between the observer (placed on $r = r_a$) and the center of the Friedmann sphere ($r = 0$).

The physical radius D_{0a} of the Friedmann sphere changes with time and forms a limit of visibility. Outside of every imaginable Friedmann sphere there is also mass, which, however, does not contribute to the gravitational events within the Friedmann sphere.
It should be mentioned that the conceivable Friedmann spheres naturally at least partially overlap.

An increasing limit distance D_{0a} decreases with time the velocity V_0 introduced above, because R_S is a constant.
Because Eq. (31) describes the physical behavior of photons in the universe, the velocity V_0 in Eq. (30) could be interpreted as an effective speed of light c_{0*}

$$V_0 = \frac{D_{0a}}{2}\sqrt{\frac{8\pi G\rho_0}{3}} = \frac{c}{2}\sqrt{\frac{R_S}{D_{0a}}} \equiv c_{0*} \quad . \tag{30a}$$

This velocity changes according to D_{0a} or ρ_0 over the time and has for us as today's observers - because of very probable $\beta_0 = 1$ - just the value of the vacuum velocity c that we can measure today.

If this interpretation is correct, the effective speed of light c_* was infinitely large at the beginning of the expansion of the universe, because at that time the Friedmann sphere was infinitely small and respectively its matter density was infinitely large. There is therefore no problem with speeds, which are apparently greater than today's speed of light, when looking into the universe

If we consider today's Hubble parameter (34) obtained above for small redshifts as a definition, we can write the redshift distance via

$$\frac{1}{\beta_0} = 2\left(\frac{c}{D_{0a}H_{0a}} - 1\right) \tag{34a}$$

also like this

$$D(z; D_{0a}, H_{0a}) = \frac{D_{0a}}{(1+z)}\left[2\left(\frac{R_H}{D_{0a}} - 1\right)\left(1 - \frac{1}{\sqrt{1+z}}\right) + z\right] \quad . \tag{31d}$$

The quotient c/H_{0a} is called the Hubble radius R_H in the literature. For this distance, the escape speed by definition reaches the speed of light if it is assumed that a linear Hubble law is valid for all distances, which is - of course - an approximation. The Eq. (31d) is therefore only valid for small redshifts how Eq. (34a).

2.3 The magnitude-redshift relation

The magnitude-redshift relation is given by the definition of the apparent magnitude m

$$m - m_{0a} = 5\log_{10}\frac{D}{D_{0a}} \quad . \tag{37}$$

Here an apparent limit magnitude m_{0a} was introduced for D_{0a}, which also changes with time. Substituting Eq. (31) into Eq. (37) then provides the sought magnitude-redshift relation

$$m(z; m_{0a}, \beta_0) = 5\log_{10}\left[\frac{1}{\beta_0}\left(1 - \frac{1}{\sqrt{1+z}}\right) + z\right] - 5\log_{10}(1+z) + m_{0a} \quad . \tag{38}$$

The two free parameters m_{0a} and β_0 can be determined by direct comparison with a magnitude-redshift diagram.

For $\beta_0 = 1$, the following simple equation results

$$m(z; m_{0a}) = 5\log_{10}\left[1 - \frac{1}{(1+z)^{3/2}}\right] + m_{0a} \quad . \tag{38a}$$

For comparison, reference is made here to Eq. (50) from Chapter 4.2, which is known from the literature.

2.4 The angular size-redshift relation

This relation results in for large distances over

$$\varphi = \arcsin\frac{\delta}{D} \approx \frac{\delta}{D} \tag{39}$$

to

$$\varphi(z;\delta/D_{0a},\beta_0)=\frac{\delta}{D_{0a}}\frac{(1+z)}{\frac{1}{\beta_0}\left(1-\frac{1}{\sqrt{1+z}}\right)+z} \quad . \tag{40}$$

In this equation φ means the measurable angular size and δ the linear size of the observed extra-galactic object.

Using $\beta_0 = 1$ we get

$$\varphi(z;\delta/D_{0a})=\frac{\delta/D_{0a}}{\left[1-\frac{1}{(1+z)^{3/2}}\right]} \quad . \tag{40a}$$

In logarithmic form Eq. (40) becomes to

$$\log_{10}\varphi(z;\delta/D_{0a},\beta_0)=\log_{10}\frac{\delta}{D_{0a}}-\log_{10}\left[\frac{1}{\beta_0}\left(1-\frac{1}{\sqrt{1+z}}\right)+z\right]+\log_{10}(1+z) \quad . \tag{41}$$

With $\beta_0 = 1$ we get the simplified equation

$$\log_{10}\varphi(z;\delta/D_{0a})=\log_{10}\frac{\delta}{D_{0A}}-\log_{10}\left[1-\frac{1}{(1+z)^{3/2}}\right] \quad . \tag{41a}$$

For comparison, reference is made to Eq. (52) from Chapter 4.2, which is known from the literature.

2.5 The number-redshift relation

In flat Euclidean space the equation for the light-path sphere becomes to

$$V=\frac{4\pi}{3}D^3 \quad . \tag{42}$$

If we introduce the redshift distance via Eq. (31)

$$V(z;D_{0a},\beta_0)=\frac{4\pi}{3}\frac{{D_{0a}}^3}{(1+z)^3}\left[\frac{1}{\beta_0}\left(1-\frac{1}{\sqrt{1+z}}\right)+z\right]^3 \tag{43}$$

we get for the number-redshift relation

$$N(z;N_{0a},\beta_0)=\frac{N_{0a}}{(1+z)^3}\left[\frac{1}{\beta_0}\left(1-\frac{1}{\sqrt{1+z}}\right)+z\right]^3 \quad , \tag{44}$$

where N_{0a} means the expected number of objects in the light-path sphere V_{0a} and besides

$$N_{0a}=V_{0a}\eta=\frac{4\pi}{3}{D_{0a}}^3\eta \qquad and \qquad N=V\eta \tag{45a, b}$$

applies. With η the number density was named. In logarithmic form results

$$\log_{10} N(z; N_{0a}, \beta_0) = 3\log_{10}\left[\frac{1}{\beta_0}\left(1-\frac{1}{\sqrt{1+z}}\right)+z\right]-3\log_{10}(1+z)+\log_{10} N_{0a} \quad . \tag{46}$$

If we here also set $\beta_0 = 1$, we get

$$\log_{10} N(z; N_{0a}) = 3\log_{10}\left[1-\frac{1}{(1+z)^{3/2}}\right]+\log_{10} N_{0a} \quad . \tag{46a}$$

For comparison, reference is made to Eq. (53) from Chapter 4.2, which is known from the literature.

3 Comparison with measurement data of astrophysics

The present paper presents a theoretical derivation of the redshift distance, which is done without approximations for e.g. small redshifts z and is therefore mainly of theoretical nature. The essay is therefore a theoretical offer to the observing cosmologists.

Nevertheless, in this chapter we will apply the theory presented here in detail to some measurement results of observational cosmology, whereby we only demonstrate the principle of evaluating the measurement data. For this reason, no more detailed error analyzes are carried out. We leave that to the experts of observational cosmology.

The cosmological relevant parameters D_{0a}, H_0, m_{0a}, M_{FS} and mean values of absolute magnitudes M (for quasars and radio galaxies) given here are therefore only to be considered as first approximations.

In data analysis, we use data that are currently available and that are partly a bit older. Every cosmological theory also has to explain these older data because they represent actual measurement results and of course do not lose their validity over time.
Of course, we are also aware that a larger number of measured values leads to more precise results for the parameters contained in the theory.

The modern ΛCDM cosmology - as the current standard model - must of course also confirm exactly these measurement results.

In our comparison between theory and measurement results of observational cosmology, we consider the three well known and above calculated classical effects of cosmology which by A. R. Sandage et al. (1995) [14] are described: magnitude-redshift relation, angular size-redshift relation and the number-redshift relation.

3.1 Magnitude-redshift diagram

The goal of any astrophysical theory is to match the measurement results of the astrophysicists as well as possible. We now want to check the magnitude of the parameters D_{0a} and β_0 introduced here. For this purpose, the magnitude-redshift diagram according to J. Huchra et al. 1983 [1] can be used as a first step, as Fig. 3. shows:

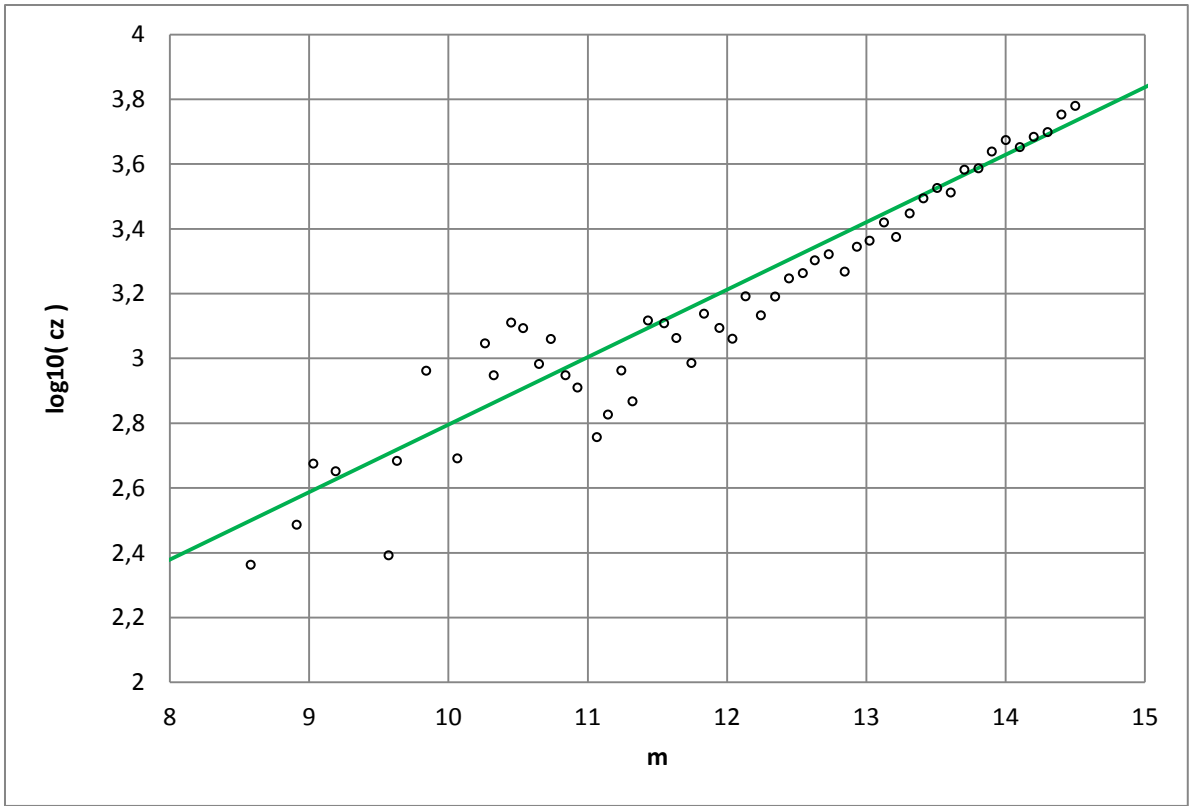

Figure 3. Magnitude-redshift diagram for 2,260 galaxies according to J. Huchra et al. (1983) [1]

Parameter: $\beta_0 = 1.0$, $m_{0a} \approx 22.62$ with a standard deviation $\sigma = 0.53717$
The black circles are mean values within 52 intervals Δm of equal size of the apparent magnitude, to which the 52 mean values of the associated redshift intervals Δz have been assigned.

The mean values used for Fig. 3. are listed in Table 2. in Chapter 4.4.

With this magnitude-redshift diagram, today's apparent limit magnitude $m_{0a} \approx 22.62$ is found for $\beta_0 = 1.0$.

Of course, other parameter combinations are possible. Which value pairs really correspond to reality must be determined by the evaluation of all astrophysical relations derived here. Here it is only a matter of explaining the principle of the evaluation.

If we succeed in finding the value of D_{0a} using m_{0a} (Eq. 37), statements can be made about the actual size of the Friedmann sphere (FS), its constant mass M_{FS}, and consequently its current matter density ρ_0.
In addition, we can then immediately deduce from the measured redshifts the associated absolute magnitudes of the objects if the cosmological redshift is considered as the only possible component of the redshift of extragalactic objects.

The prerequisite for the determination of the parameters mentioned is to find at least one extra-galactic object which is located exactly on the theoretical curve with the parameter pair $\beta_0 = 1.0$ and $m_{0a} = 22.62$ and whose absolute magnitude M is known. For this purpose, the literature was reviewed and the following objects were found:

object	cz [km/s]	$\log_{10}(cz)$	m	M	reference
M100 = NGC 4321	1560	3.1931	10.26	-20.9	[2]
M96 = NGC 3368	899	2.9538	10.32	-20	[3]
NGC 4571	343	2.5353	12.09	-18.82	[4]
IC 4182	339	2.5302	9.55	-19.92	[5]
mean value object	785.3	2.8950	10.56	-19.91	

Table 1. Some galaxies with known absolute magnitude

Measurements not found in the cited literature were taken from the articles by J. Huchra et al. (1983) [1], R.C. Kraan-Korteweg et al. (1979) [6] and A. Sandage et al. (1975) [7].

Unfortunately, all of these galaxies are not lying on the theoretical curve using the pair of parameters used above. But averaging results fortunately in an object that is at least very close to the curve, as shown in Fig. 4.:

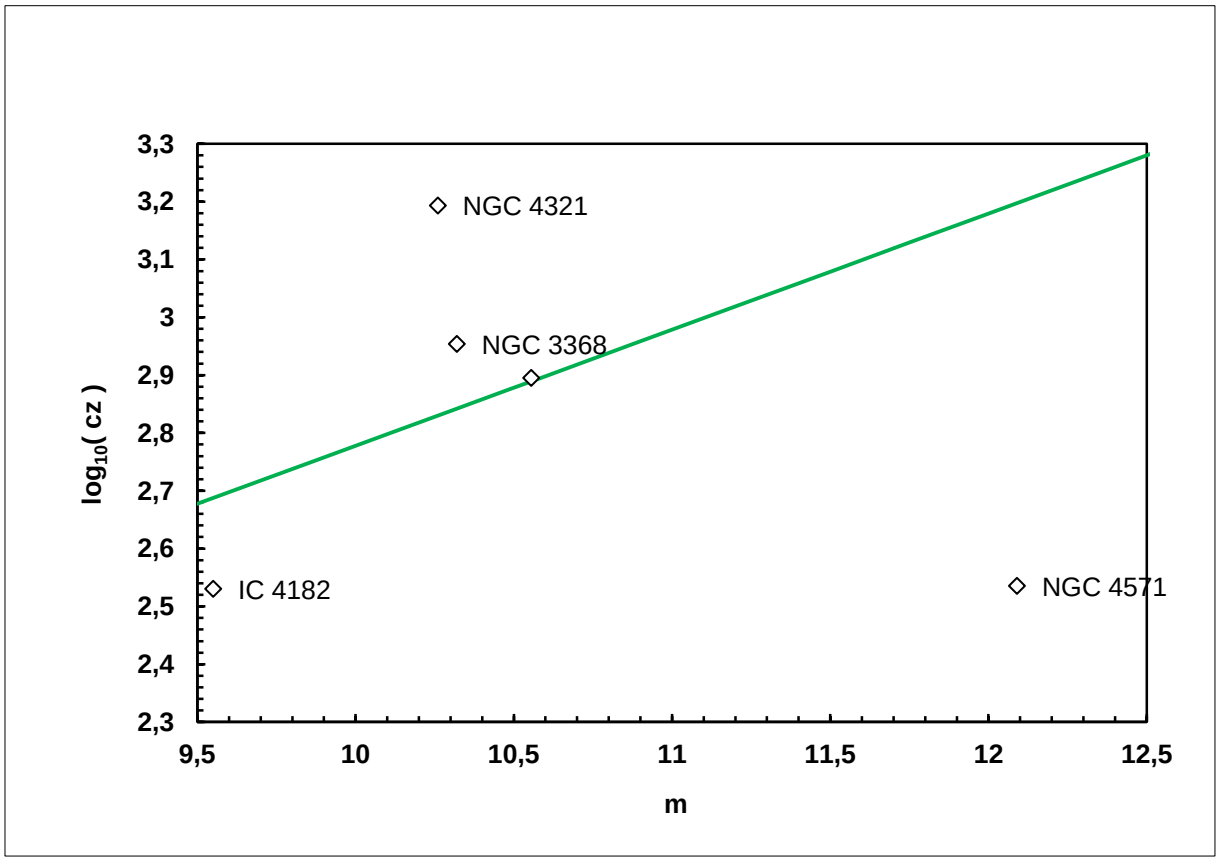

Figure 4. Magnitude-redshift diagram for the galaxies NGC 4321, NGC 4571, NGC 3368 and IC 4182
Parameter: $\beta_0 = 1.0$, $m_{0a} \approx 22.62$ with a standard deviation $\sigma = 0.02909$

The absolute magnitude of the mean value object yields $D_{0a} = 3{,}206$ Mpc when the equation

$$D_{0a} = 10^{\frac{m_{0a}-M}{5}+1} \tag{47}$$

is used. This result provides today's Hubble parameter $H_{0a} = 62.34$ km/(s * Mpc) and the associated current Hubble time $t_{0a} = 15.7 * 10^9$ years, which fits well with the age of the oldest globular star clusters. With $\beta_0 = 1$ the Schwarzschild radius $R_S = 4D_{0a} = 12{,}824$ Mpc results and from this the mass of the Friedmann sphere to $M_{FS} = 2.67 * 10^{56}$ g.

If we consider D_{0a} as the radius of the Friedmann sphere, its current mass density results in $\rho_{0FS} \approx 6.57 * 10^{-29}$ g/cm^3. This density is actually much higher than today's radiation density with $\rho_{0R} \approx 7.80 * 10^{-34}$ g/cm^3. This actually justifies neglecting the radiation density when deriving the redshift distance afterwards.

Now a few words to the curvature of the theoretical curve for large redshifts follow. One of the original goals in finding the right Hubble law was the poor consistency of the textbook theory with the magnitude-redshift diagrams of quasars. Fig. 5. shows such a diagram for the quasar data according to Véron-Cetty (2003) [8] and the radio galaxy data of A. Sandage (1972) [9].

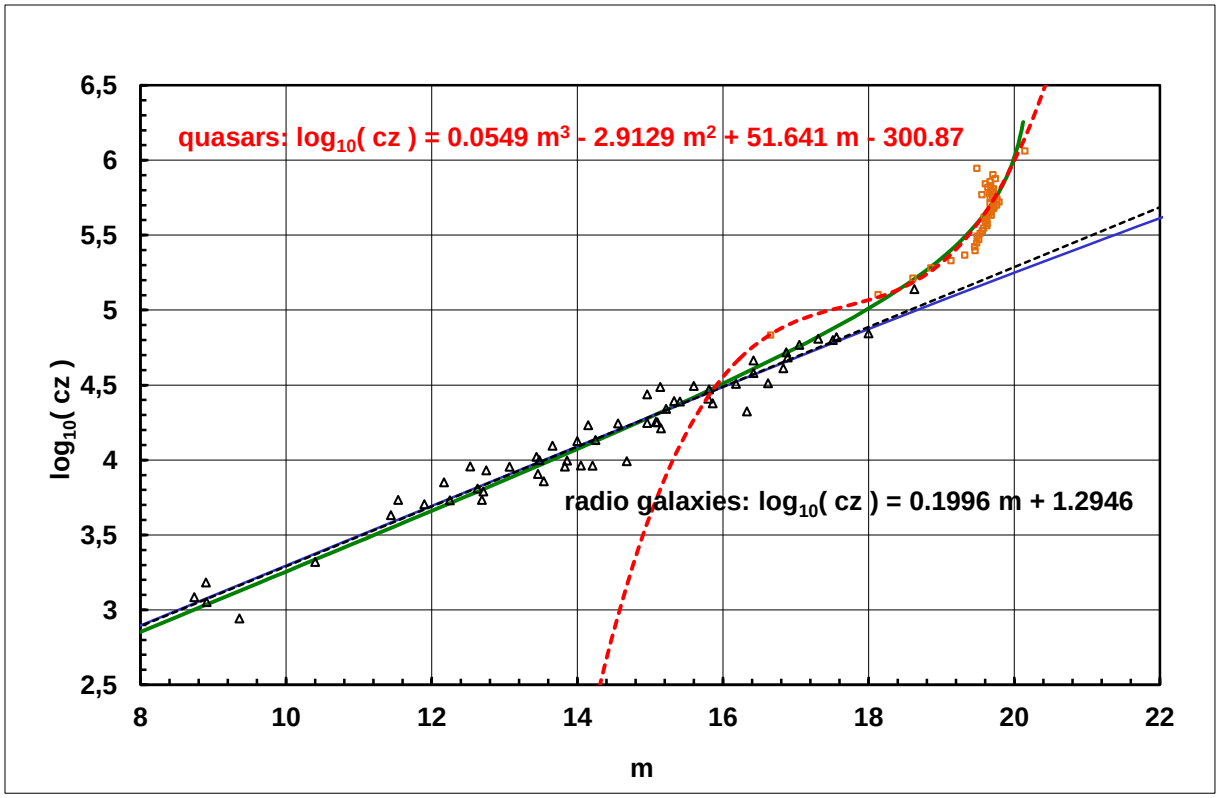

Figure 5. Magnitude-redshift diagram for the mean values of quasars (Véron-Cetty, 2003) [8] and radio galaxies (Sandage 1972) [9] in comparison with the textbook theory (blue curve) and the theory presented here (green curve)

Parameter: $\beta_0 = 1.0$, $\langle M_Q \rangle \approx -22.29$ with a standard deviation $\sigma = 0.19415$, $m_{0aQ} \approx 20.24$ and $D_{0a} \approx 3{,}206$ Mpc

Because the cosmological redshift z generally only depends on the distance (the light path traveled by the photons) of the observed cosmic objects [Eq. (31)] but the apparent magnitude m depends on the light path and on the absolute magnitude M of the objects, the redshift in averaging for large data sets is generally to be regarded as primary. For this reason, we first formed 45 redshift intervals Δz for the total number of 48,690 quasars, each with an equal number of quasars (n = 1082). This procedure ensures good statistics even for the smallest and largest redshifts.

Corresponding intervals of the apparent magnitude Δm_i belong to these redshift intervals Δz_i ($1 \leq i \leq 45$). We calculated the mean values $\langle z_i \rangle$ and $\langle m_i \rangle$ in both intervals. These mean values are shown in Fig. 5. as yellow squares. The list of mean values can be found as Table 3. in Section 4.4.

The curved solid line (green) corresponds to the magnitude-redshift relation derived here, which has been adjusted within in the curved area with $\langle M_Q \rangle \approx -22.29$ to the interval mean values of the quasars (yellow squares). The straight line drawn (blue) corresponds to the textbook theory. It was adapted to the radio galaxies (black triangles). The straight dotted line (black) is the best curve through the radio galaxies. The other dotted curved line (red) is a best-fit curve only by the averages of the quasars, whose equation is also shown in the figure above.
The quasars with about $\langle M_Q \rangle \approx -22.29$ on average are slightly fainter than the radio galaxies used here for comparison, for which $\langle M_{RG} \rangle \approx -22.8$ is found. The quasars are therefore less absolute bright than previously thought.

It turns out that the average value pairs of 48,690 quasars can be described best with $\beta_0 = 1$. This is also the deeper reason why for the determination of m_{0a} using the magnitude-redshift diagram according to J. Huchra (1993) [1] $\beta_0 = 1$ has been chosen.
If $\beta_0 = 1$ is accepted as correct, it follows that the current effective speed of light $V_0 = c_{0*}$ [Eq. (30a)] is exactly equal to the speed of light c_0 which is measurable today! This result would be immediately obvious.

The theory presented here is able to explain correctly the average locations of the quasars in the magnitude-redshift diagram and to eliminate their previously assumed magnitude problem.

3.2 Angular size-redshift diagram

We use further the parameter choice $\beta_0 = 1$ and $m_{0a} = 22.62$ and consider the angular size-redshift diagram according to K. Nilsson (1993) [10], which is shown in Fig. 6.:

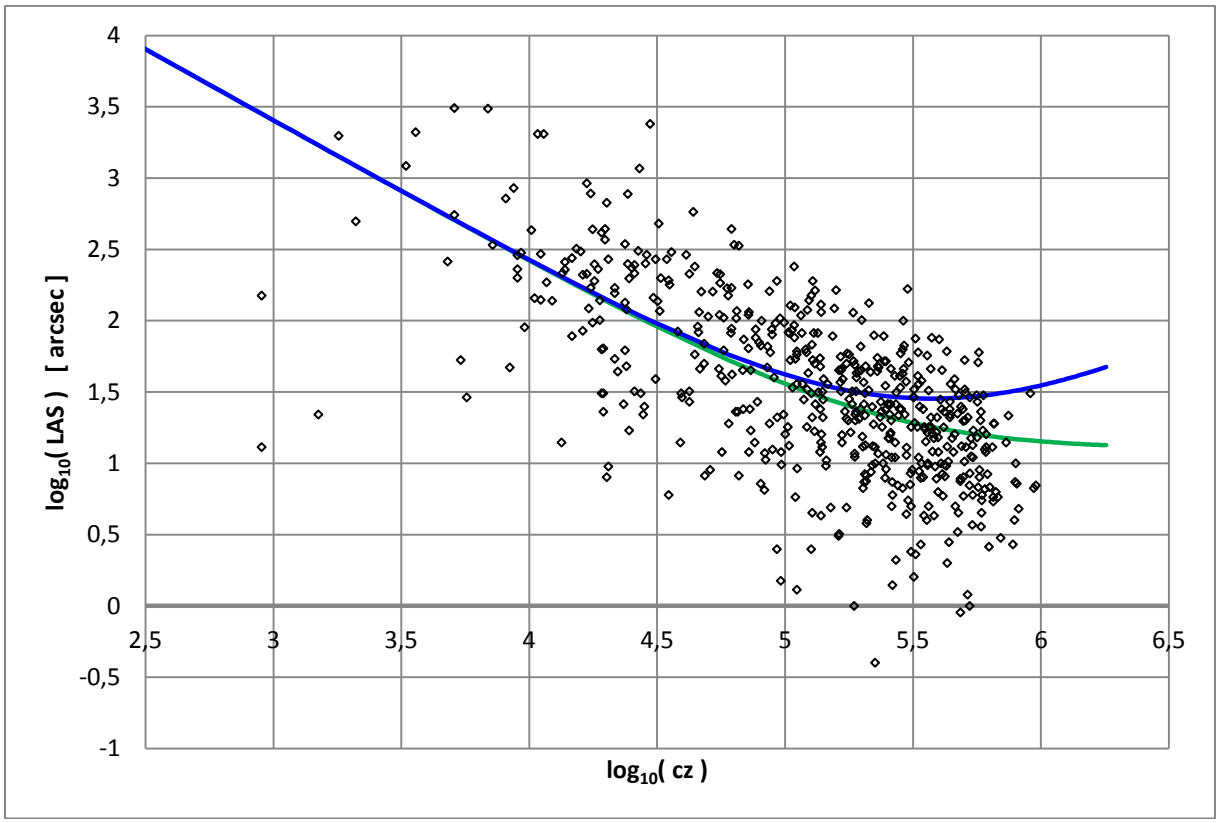

Figure 6. Angular size-redshift diagram according to K. Nilsson et al. (1993) [10]

Parameter: $\beta_0 = 1.0$, $(\delta/D_{0a}) \approx 6.14 * 10^{-05}$ with a standard deviation $\sigma = 0.00378$ within the linear part of the curve, $D_{0a} \approx 3{,}206$ Mpc and $\delta \approx 0.197$ Mpc
No mean values were formed making this diagram.

The result for the quotient $\delta/D_{0a} \approx 6.14 * 10^{-5}$. This means an average linear size of the objects of $\delta \approx 0.197$ Mpc if $D_{0a} \approx 3{,}206$ Mpc is assumed.
The picture shows that the textbook theory for the flat Euclidean space [Eq. (52)], the upper curved curve (blue), fits less well with the measured values than the theory presented here (green).

3.3 Number-redshift diagram

Again we choose $\beta_0 = 1$ and $m_{0a} = 22.62$ to evaluate the following number-redshift diagram.

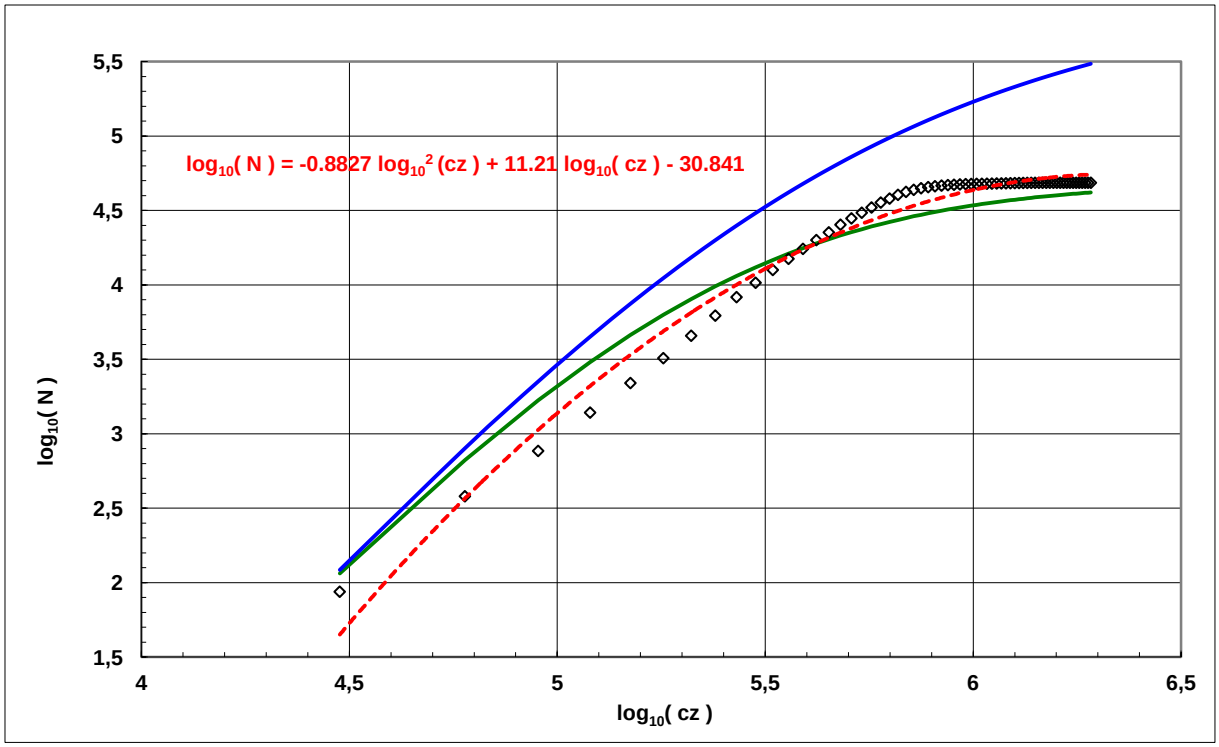

Figure 7. Number-redshift diagram for 48,690 quasars according to M.-P. Veron-Cetty (2003) [8]

Parameter: $\beta_0 = 1.0$ with a standard deviation $\sigma = 0.14564$ and $N_{0a} =$ **48,690**

The measuring points shown in Fig. 7. correspond to the summation of the number of quasars within 64 redshift intervals of equal size. In chapter 4.4 (mean value tables) the details are given.

For the sake of simplicity, $N_{0a} = 48{,}690$ has been chosen in this figure, which is exactly the number of quasars in the catalog of Véron-Cetty (2003) [8] for which the redshift is given there.

The upper curve (blue) again corresponds to the theory for the flat Euclidean space from the literature [Eq. (53)], while the lower solid curve (green) represents the number-redshift relation derived here. The dotted curve (red) is a best-fit curve whose formula is also shown within the diagram.

The theory from the literature expects almost 10 times the number of quasars for large redshifts compared to the theory presented here. That is certainly wrong.

The fact that the theory and the measurement data do not agree exactly may be due to the fact that developmental effects could play a role (e.g. the existence or nonexistence of temporally first quasars for large redshifts and temporally last quasars for small redshifts), but such effects have not been considered in the derivation of Eq. (46) given here.

In addition, it must be assumed that the measurement data are incomplete: The measurements probably do not extend far enough into the redshift space and some of them certainly do not take into account existing quasars in different directions, this means in summery they do not cover the whole space.

4 Additions

4.1 About the mass of Friedmann sphere

The cause of the expansion of the universe visible to us as observers is its constant mass M or the time-varying density $\rho_M(t)$, respectively. It ensures that the scale parameter changes over time. To check this statement, simply set the matter density in the Friedmann equation to zero.

Every cosmologist therefore has to ask himself where exactly this mass is located in the universe. He can gain an answer for this by borrowing the appropriate ideas from classical non-relativistic Newtonian cosmology. There he has to imagine a mass sphere whose radius changes over time (e.g. grows). This means that the mass in question is completely within this sphere, and it is evenly distributed and remains there according to the cosmological principle. In relativistic cosmology, the time depend product of scale parameter and coordinate distance R(t) = a(t) r takes over the role of the physical radius of the mass sphere, and it holds that the entire mass to be considered is inside this sphere (Friedmann sphere named here).
Incidentally, the Friedmann equation of the flat universe looks strangely exactly as the equation of the non-relativistic Newtonian cosmology. There is no relativity seen in the equation e.g. in the sense of limiting the rate of change da/dt of the scale parameter to the speed of light.

The Fig. 8. shows the projection of a Friedmann sphere in to the plane at time t_0 (today) in which examples of possible places for an observer and galaxy observed are drawn.

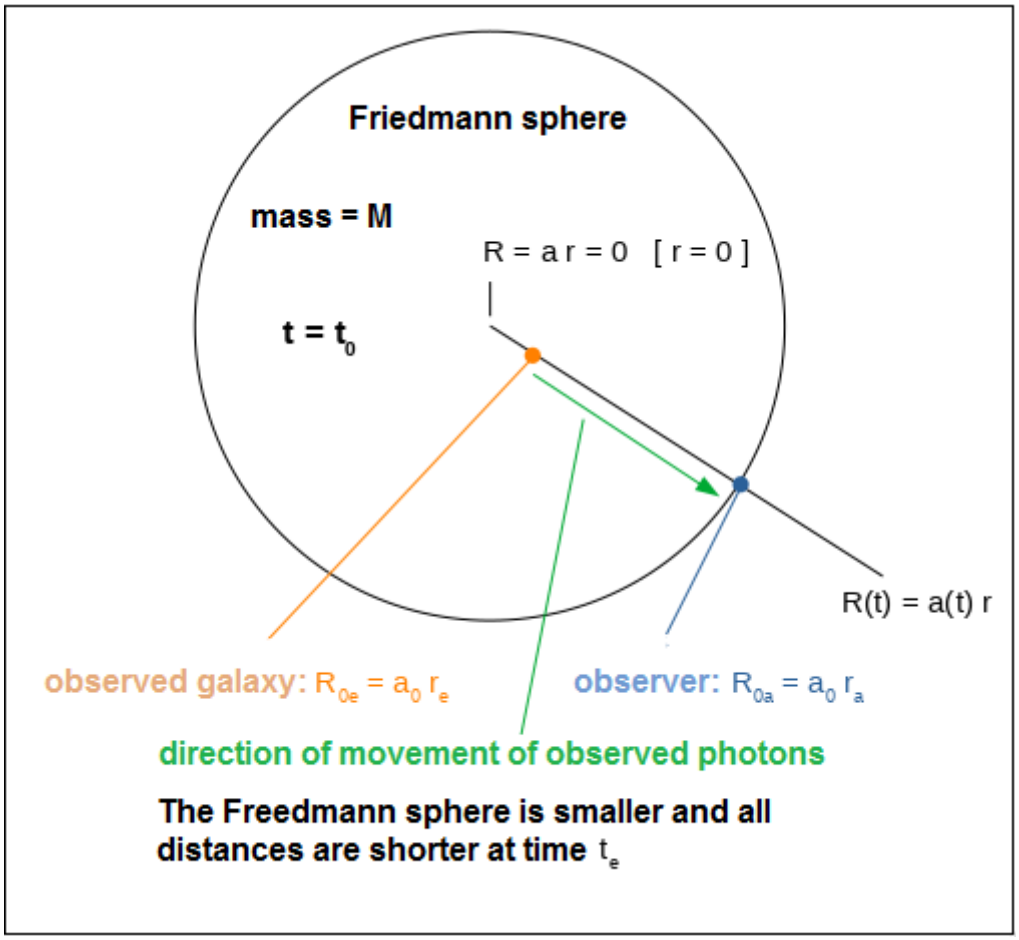

Figure 8. Friedmann sphere with examples of physical locations of an observer and a galaxy

Because of the law of conservation of mass

$$M = \frac{4\pi}{3}\rho_0 {a_0}^3 {r_a}^3 = \frac{4\pi}{3}\rho_0 {D_{0a}}^3 \tag{36a}$$

which is used here we see that D_{0a} is today's radius of the Friedmann sphere with today's mass density ρ_0.

An observable galaxy can minimally have the co-moving coordinate with $r_e = 0$. If a galaxy is placed there, we observe an infinitely large redshift for such a galaxy according to our redshift distance. For all other locations $r_e \neq 0$ of an observed galaxy, a smaller redshift is always measured.

Because an infinitely large redshift is always observed for the light path $D = D_{0a}$, it can be assumed that in the physical radius $D_{0a} = a_0 r_a$ of a Friedmann sphere, the co-moving coordinate r_a has the maximum possible value $r = 1$ according to the complete FLRWM. D_{0a} therefore describes the maximum size of the Friedmann sphere, which of course is time-dependent. This maximum value of the co-moving and dimensionless radial coordinate r follows from the FLRWM with positive curvature $\varepsilon = 1$ and, from our point of view, can theoretically not simply be neglected despite the flat space-time assumed for today's universe.

Of course, each observer can also e.g. look in exactly the opposite direction to the direction shown (green arrow). In this case, he looks again into a Friedmann sphere, which belongs to this direction. For $D = D_{0a}$ there is also an infinite redshift in this direction. The observer can of course also look in any other directions. The observer always looks into Friedmann spheres, which of course partially overlap.
Overall, there is a part of the universe with a spherical radius D_{0a}, that is visible to any observer. A universe thought to be spherical corresponds to at least one sphere with the radius $2 * D_{0a}$, since beyond D_{0a} there is always also mass. Every observer sits on the surface of Friedmann spheres. Nevertheless, he can believe that his place is also in a center of such a Friedmann sphere.

If we would put the position of an observer a little outside the Friedmann sphere shown in Fig. 8., he would find the same situation as described above, if the universe would be actually much larger than a sphere with the radius $2 * D_{0a}$ or even infinitely large.

4.2 About the derivation of the redshift distance in the literature

In the literature, the observer is usually placed in the coordinate origin $r_a = 0$ (see Fig. 9.). Because of $r_e \geq r_a = 0$, this results in the light path simply as $D_{literature} = a_0 r_e$. This depends only on the co-moving coordinate location r_e of the observed galaxy and on the today's value of the scale parameter a_0. An earlier scale parameter such as a_e does not play a role in this approach, which we consider as a strong limitation of the generality.

In this case, the photons run inside a mass sphere from the outside to the inside, i.e. always towards the origin $r_a = 0$ (incoming photons). Any other way of defining $D_{literature}$ would be physically nonsense.

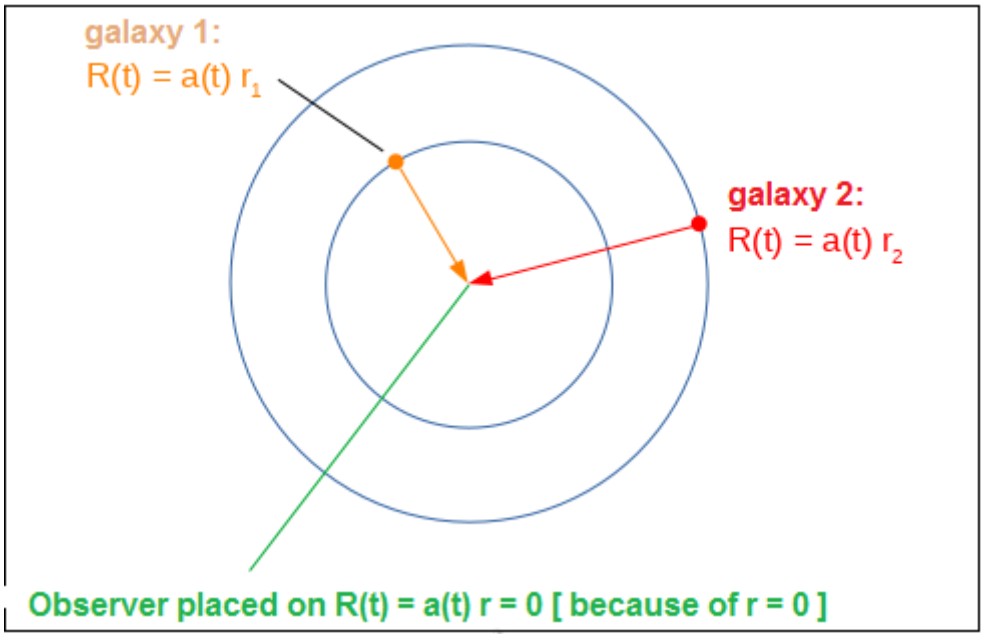

Figure 9. Observer generally placed on the center of the co-moving coordinate system ($r_a = 0$)

The calculation analogous to our derivation of the redshift distance (see chapter 2.2) results first in

$$D_{literature}(z; a_0, R_S) = D_0 \frac{\left(1+z-\sqrt{1+z}\right)}{(1+z)} \qquad with \qquad D_0 = 2a_0\sqrt{\frac{a_0}{R_S}} \quad . \tag{48}$$

We have denoted the index of the maximum distance for which z = ∞ is reached with 0, because the calculation based on $D_{literature,\,i} = a_0\, r_{e,\,i}$ generally gives the today's distance between any galaxy i and any observer.

In the literature, the magnitude distance is indicated with

$$D_m = (1+z)D_{literature} \quad , \tag{49}$$

whereby with the help of factor (1 + z) an overall thinning of the number of photons due to the enlargement of the spherical area on which the radiation hits after its way through the universe and the energy loss due to the redshift is taken into consideration.

So it results first in

$$D_m(z; a_0, R_S) = 2\,a_0 \sqrt{\frac{a_0}{R_S}}\left(1+z-\sqrt{1+z}\right) \tag{50}$$

or

$$D_m(z; a_0, R_S) = 2\,a_0 \sqrt{\frac{a_0}{R_S}}(1+z)\left(1-\frac{1}{\sqrt{1+z}}\right) \quad . \tag{50a}$$

Here, too, the prefactor is a distance parameter for which can be introduced an apparent magnitude.

If, in a case which is also possible, the observed galaxy (each one because there are many; see Fig. 10.) each placed to its own coordinate origin (outgoing photons), the result of calculation - for obvious reasons of symmetry - is of course the same redshift distance as above. This can easily be checked by means of an elementary calculation.

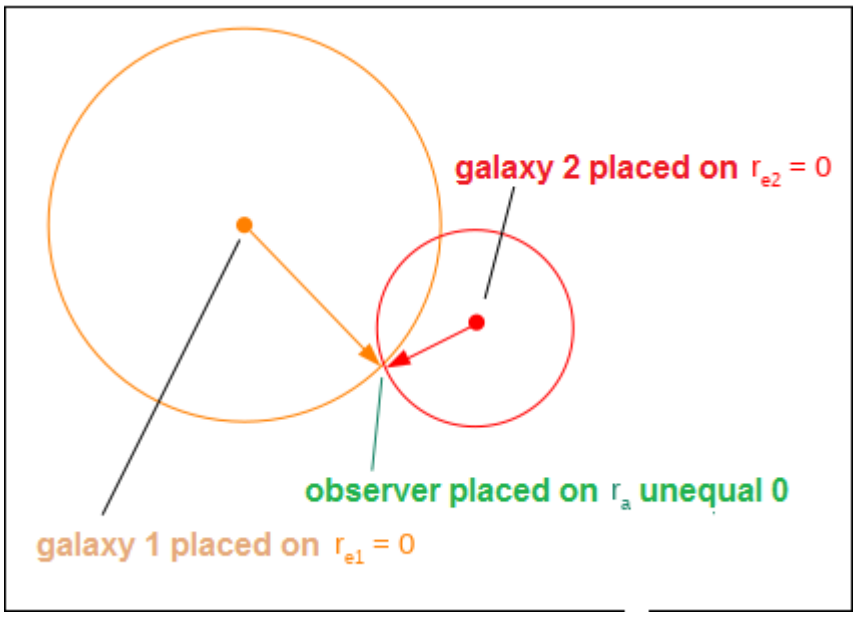

Figure 10. Observed galaxies (i = 1, 2) each in their own coordinate origin ($r_{e\,i} = 0$)

Therefore, this results for the magnitude-redshift relation in

$$m_{literature}(z; m_{D_0}) = 5\log_{10}\left(1-\frac{1}{\sqrt{1+z}}\right) + 5\log_{10}(1+z) + m_{D_0} \quad . \tag{51}$$

For the angular size-redshift relation we find

$$\log_{10}\varphi_{literature}(z;\,\delta/D_0)=\log_{10}\frac{\delta}{D_0}-\log_{10}(1+z)-\log_{10}\left(1-\frac{1}{\sqrt{1+z}}\right)\quad . \tag{52}$$

For the number-redshift relation we get accordingly

$$\log_{10} N_{literature}(z;N_0)=3\log_{10}\left(1-\frac{1}{\sqrt{1+z}}\right)+3\log_{10}(1+z)+\log_{10} N_0\quad . \tag{53}$$

All three equations also result from the well-known Mattig equation (1958), if the delay parameter $q_0 = ½$ is set there, whereby this equation describes a flat universe (see e.g. Sandage, A. R. et al. [11]).

We have used Eq. (51), Eq. (52) and Eq. (53) in the measured value diagrams for comparison with the theory presented here.

4.3 Consideration of the radiation density in the early days of cosmological expansion

When deriving the redshift distance in Chapter 2.2, we neglected the relativistic radiation density ρ_R that was originally dominant in the early days of the universe. The reason for this is that today, actually for several billion years, this density no longer plays a role in the further development of the universe over time due to its small value compared to the non-relativistic mass density ρ_M.

If this radiation density is taken into account from the start when deriving the redshift distance according to the scheme in chapter 2.2 the result is a more complex redshift distance because it then also dependent on a further parameter:

$$D_{RM}(z;D_{0a},\beta_{0,M},\Omega_{0,RM})=\frac{D_{0a}}{(1+z)}\left\{\frac{1}{\beta_0}\left[\sqrt{1+\Omega_{0,RM}}-\sqrt{\Omega_{0,RM}+\frac{1}{(1+z)}}\right]+z\right\}\quad .$$

$$with\qquad D_{0a}=a_0 r_a\qquad and\qquad \frac{1}{\beta_{0,M}}=2\sqrt{\frac{D_{0a}}{R_S}}\qquad and\qquad \Omega_{0,RM}=\frac{\rho_{0,R}}{\rho_{0,M}} \tag{54}$$

$$index\ 0:today\qquad index\ R:radiation\qquad index\ M:non-relativistic\ matter$$

Here the current density quotient $\Omega_{0,RM}$ is included as a further parameter, which takes into account the very early radiation era. For today's radiation density, the designation $\rho_{0,R}$ was introduced again and today's non-relativistic mass density was named $\rho_{0,M}$. The Parameter $\beta_{0,M}$ corresponds to our parameter β_0 in Eq. (31).

With the numerical values for today's density quotient $\Omega_{0,RM}$ mentioned in chapter 1 it can be seen immediately that $\rho_{0,R}$ or $\Omega_{0,RM}$ can actually be neglected.

In addition, when comparing Eq. (54) with the measured values (e.g. magnitude-redshift diagram of the quasars), there is no longer any effect fitting the measurement curve for a density quotient smaller then $\Omega_{0,RM} \approx 0.01$.

If we set $\Omega_{0,RM} = 0$ in Eq. (54) - this corresponds to our neglect of today's radiation density $\rho_{0,R}$ - we get Eq. (31) again. Accordingly, this Eq. (31) is actually valid as today's redshift distance, containing the parameters D_{0a} and $\beta_{0,(M)}$ only.

4.4 Mean value tables

We also state here the data sets (mean value formation) used by us for the evaluation of cosmological relevant measurement data in order to offer a verification option.

I) Data set from J. Huchra et al. (1983) [1]

This data set is limited to m = 14.5 with regard to the apparent magnitude. Therefore, we have formed 52 equal intervals of the apparent magnitudes and calculated the mean values <m>. Than we assigned the mean values <z> of the redshift to these mean values. The result is shown in Table 2..

interval	< z >	< m >	interval	< z >	< m >	interval	< z >	< m >	interval	< z >	< m >
1	0,02011	14,500	14	0,00792	13,214	27	0,00415	11,945	40	0,00321	10,650
2	0,01891	14,401	15	0,00878	13,127	28	0,00459	11,835	41	0,00414	10,536
3	0,01669	14,301	16	0,00771	13,023	29	0,00323	11,744	42	0,00431	10,450
4	0,01613	14,202	17	0,00739	12,932	30	0,00386	11,636	43	0,00296	10,325
5	0,01500	14,102	18	0,00619	12,845	31	0,00429	11,548	44	0,00372	10,262
6	0,01577	14,001	19	0,00700	12,730	32	0,00437	11,432	45	0,00164	10,063
7	0,01453	13,901	20	0,00671	12,630	33	0,00246	11,321	46	0,00306	9,840
8	0,01290	13,805	21	0,00612	12,544	34	0,00307	11,241	47	0,00161	9,630
9	0,01277	13,704	22	0,00590	12,445	35	0,00224	11,145	48	0,00082	9,570
10	0,01086	13,606	23	0,00518	12,345	36	0,00191	11,065	49	0,00150	9,190
11	0,01122	13,509	24	0,00454	12,243	37	0,00272	10,926	50	0,00158	9,030
12	0,01042	13,410	25	0,00519	12,133	38	0,00296	10,840	51	0,00102	8,910
13	0,00936	13,311	26	0,00384	12,038	39	0,00383	10,735	52	0,00077	8,580

Table 2. Averaging for the data set of J. Huchra et al. (1983) [1]

These data were used making Fig. 3..

II) Data set of Véron-Cetty, M.-P. & Véron P. (2003) [8]

IIa) Magnitude-redshift diagram

Because of the large number of quasars within this data set we first formed 45 redshift intervals with 1,082 quasars each (a total number of 48,690 quasars) and calculated the corresponding redshift mean values <z>. We then calculated the associated mean values <m> of the apparent magnitude. The result is shown in Table 3..

interval	< z >	< m >	interval	< z >	< m >	interval	< z >	< m >
1	0,22781	16,655	16	1,26497	19,629	31	1,88573	19,671
2	0,42411	18,131	17	1,30822	19,604	32	1,92566	19,703
3	0,54586	18,61	18	1,35045	19,624	33	1,96734	19,557
4	0,63882	18,856	19	1,39277	19,587	34	2,01270	19,656
5	0,71446	19,132	20	1,43575	19,686	35	2,06101	19,702
6	0,77836	19,321	21	1,47938	19,658	36	2,10707	19,678
7	0,83364	19,463	22	1,51873	19,682	37	2,15417	19,716
8	0,88507	19,456	23	1,55518	19,687	38	2,20282	19,638
9	0,93860	19,486	24	1,59433	19,718	39	2,25829	19,678
10	0,99056	19,515	25	1,63636	19,723	40	2,32477	19,604
11	1,04083	19,491	26	1,67718	19,76	41	2,40868	19,669
12	1,08687	19,533	27	1,71901	19,669	42	2,51872	19,741
13	1,13313	19,564	28	1,76149	19,792	43	2,67596	19,708
14	1,17863	19,581	29	1,80252	19,715	44	2,95107	19,488
15	1,22118	19,626	30	1,84408	19,764	45	3,85371	20,147

Table 3. Averaging the data set by Véron-Cetty, M.-P. & Véron P. (2003) [8]

These data were used making Fig. 5..

IIb) Number-redshift diagram

To create this diagram, we first formed 64 redshift intervals of equal size and then calculated the associated numbers of quasars within these z intervals. The result is shown in Table 4..

z-interval upper limit	N	z-interval upper limit	N	z-interval upper limit	N	z-interval upper limit	N
0,1	88	1,7	2.612	3,3	150	4,9	15
0,2	295	1,8	2.565	3,4	81	5	10
0,3	388	1,9	2.589	3,5	45	5,1	4
0,4	623	2	2.620	3,6	44	5,2	3
0,5	805	2,1	2.283	3,7	91	5,3	1
0,6	1.031	2,2	2.276	3,8	87	5,4	0
0,7	1.340	2,3	1.883	3,9	78	5,5	1
0,8	1.666	2,4	1.379	4	57	5,6	1
0,9	2.063	2,5	1.076	4,1	76	5,7	0
1	2.065	2,6	774	4,2	72	5,8	1
1,1	2.271	2,7	626	4,3	65	5,9	1
1,2	2.376	2,8	454	4,4	56	6	1
1,3	2.491	2,9	365	4,5	50	6,1	1
1,4	2.556	3	271	4,6	21	6,2	0
1,5	2.542	3,1	249	4,7	18	6,3	2
1,6	2.834	3,2	187	4,8	14	6,4	1

Table 4. Number N of quasars within redshift intervals of equal size in the data set of Véron-Cetty, M.-P. & Véron P. (2003) [8]

These data were used making Fig. 7..

References

[1] Huchra, J.; Davis, M.; Latham, D. and Tonry, J.:
The Astrophysical Journal Supplement Series, 52 (1983), p.89

[2] Freedman, W. L., et al., 1994, Nature, 371, 757

[3] Tanvir, N. R., Shanks, T., Ferguson, H. C. and Robinson, D. R. T., 1995, Nature, 377, 27

[4] Pierce, M. J.; Welch, D. L.; McClure, R. D.; van den Bergh, S.; Racine, R. and Stetson, P. B.:
1994, Nature 371, 385

[5] Sandage, A.; Saha, A.; Tammann, G. A.; Panagia, N. and Macchetto, D.:
The Astrophysical Journal, 401 (1992), L7

[6] Kraan-Korteweg, R. C. and Tammann, G. A.:
Astronomische Nachrichten 300 (1979), Heft 4, S.181

[7] Sandage, A. and Tammann, G. A.:
The Astrophysical Journal, 196 (1975), p.313

[8] Véron-Cetty, M.-P. & Véron P.:
"A Catalogue of Quasars and Active Nuclei", 11th edition, August 2003, http://www.obs-hp.fr

[9] Sandage, A.:
The Astrophysical Journal, 178 (1972), p.25

[10] Nilsson, K.; Valtonen, M. J.; Kotilainen, J. and Jaakkola, T.:
The Astrophysical Journal, 413 (1993) p.453

[11] Sandage, A.; Kron, R.G. and Longair, M. S.: The Deep Universe, Springer-Verlag, 1995,
(Saas-Fee Advanced Course 23, Lecture Notes 1993, Swiss Society for Astrophysics and Astronomy,
Publishers: Binggeli, B. and Buser, R.)

[12] The Planck Collaboration: Planck 2018 results. VI. Cosmological parameters, arXiv:1807.06209